J. Condensed Matter Nucl. Sci. 39 (2025) 105–129

Research Article

Effects of Electric Pulse Shape on AHE Generation in High-Temperature Surface-Modified Constantan under Hydrogen and Deuterium Gases

F. Celani, P. Cerreoni

Istituto Nazionale di Fisica Nucleare, Via E. Fermi 56, 00044 Frascati, Italy

C. Lorenzetti, E. Purchi, S. Cupellini, M. Nakamura

International Society of Condensed Matter Nuclear Science (ISCMNS_L1), Via Cavour 26, 03013 Ferentino, Italy

G. Vassallo

Engineering Department, University of Palermo , 90128 Palermo, Italy

U. Mastromatteo

ARGAL, Via S. Stefano 27B, 2008 Bareggio, Italy

Abstract

This paper is a concise summary of our research, as presented at the conference ICCF25 (27–31 August 2023, Radisson Blu Hotel, Szczecin, Poland), and also includes content previously shared at the Workshop ANV12 (17–19 February 2023, Terni, Italy). Since 1994, our research has centered on exploring the impact of electric pulse shapes on generating Anomalous Heat Effects (AHE) in various materials within diverse gas environments. Initially, we observed these effects in Pd and Pd-Y alloys using unipolar pulsing in electrolytic conditions [1], [2]. However, the inherent limitations of this setup, including a maximum solution temperature of approximately 100 °C at 1 bar pressure, posed challenges for substantial progress and replication by fellow researchers. More recently, we revisited the pulse approach [3], [4], this time employing cost-effective Constantan wires, which are significantly more budget-friendly than Pd. In several experiments, we shaped these wires in a manner akin to our previous Pd experiments, and operated in gas environments encompassing H_2, D_2, or mixtures involving low thermal-conductive gases such as Ar or Xe. This setup enabled wire temperatures of up to 850 °C, which offered significant benefits in terms of recovering excess energy at the reactor's external surface. We simplified our pulsing circuitry by leveraging the 50 Hz power line and fast, high-power diodes. Unlike previous experiments, which used capacitive discharge with negative polarity between the active wire and the counter electrode, we now explore the effects of positive pulses, bipolar waves, and DC polarization.

Our findings, presented at the Multidisciplinary Workshop ANV12 in February 2023, confirm the superior efficacy of negative pulses at 50 Hz. While positive pulses and bipolar waves also produced beneficial effects compared to DC polarization, their ability to induce Anomalous Heat Excess (AHE) was notably weaker, with AHE values up to three times lower.

 ISSN 2227-3123

In addition, we have streamlined our experimental approach by testing pristine wires, departing from traditional surface pre-treatment methods. The overview of our experiments also encompasses the investigation of the effects of specific powders surrounding the wire, as well as the critical role of Super Abundant Vacancies (SAVs). These SAVs represent a localized bulk effect generated through prolonged electromigration. This phenomenon, first suggested by Prof. M. Staker, builds on the pioneering work of Prof. Y. Fukai [5].

Looking beyond the ANV12 Workshop, we aim to share results from these simplified setups and future tests. It is worth noting that this project is primarily funded by the European Union's Horizon 2020 research and innovation program, under grant agreement no. 951974, as part of the "CleanHME" project.

Keywords: LENR, AHE, solid state fusion, deuterium, hydrogen, constantan, wires, nickel, electric pulses, pulsed currents.

1. Main Results Presented at ANV12 (14 February 2023)

Our presentation at ANV12 revealed a series of significant findings, marking a crucial phase in our experimental exploration. The journey commenced with the treatment of virgin wire, where a succession of physical-chemical treatments aimed at enhancing its specific surface area was implemented [6]. In its untreated state, our Constantan wire has a surface area of approximately 10 cm^2, with a diameter of 200 μm and a length of 158 cm. The reactor design utilized in this phase is based on the innovative "inverse coaxial coil" concept, which has been in development since 2019 [4], [7], [8], [9]. This design was developed after extensive trial and error involving various reactor core constructions. The complexities of this design are clearly illustrated in Figs. 1 and 2. Notably, the wire withstood over 28 full cycles, experiencing a wide temperature range from approximately 800 °C to room temperature (RT).

The experimental timeline unfolded from October 11, 2022, to February 13, 2023. Unfortunately, the wire eventually succumbed to breakage, primarily attributed to operational errors during a test of novel electrical circuitry. The overarching goal of this circuitry was to minimize "wasted" input power, fostering optimism for increased generation of Anomalous Heat Effects (AHE).

In an important experiment conducted during this time, Constantan wire was immersed in sub-micrometric powders composed of Cu-Ni-Fe, which served as the primary active material for hydrogen absorption. Additionally, oxides of Ca-Sr-Ba were included to function as Low Work-Function materials for electron emission at temperatures above 500 °C. The composition of these powders closely resembled that of the treated primary wire surface, addressing the vulnerability of previous setups to catastrophic wire failures, especially under brief, high-temperature conditions.

Our goal was to elevate the wire's temperature beyond the limits set by Ohm's law through injected electric power. Constantan, known for its nearly constant resistivity over a wide temperature range (approximately -50 to $+700$ °C), is particularly susceptible to changes in resistivity due to hydrogen absorption, which can complicate electromigration phenomena where maximizing ΔV/cm values is essential.

Localized hot spots, which we hypothesize to be the primary sources of Anomalous Heat Excess (AHE), likely contribute to the rise in the wire's temperature. However, if these hot spots surpass $\sim$1200 °C, the wire may fuse, prematurely terminating the experiment. To prevent this, continuous monitoring of the wire's resistance is essential to accurately assess the operating conditions and optimize the AHE phenomenon. Developing a robust procedure to manage this critical aspect during extended reactor operations was imperative. The similarity in composition between the powders and the primary active material (Constantan wire and its coating) suggests that they could significantly contribute to the manifestation of AHE.

To ensure a precise energy balance while varying input power, we implemented "thermometry" for quicker measurements compared to traditional flow calorimetry. This approach required reference and calibration runs at the beginning of experiments before introducing any active gases such as H_2 or D_2. This strategy not only improves experimental efficiency but also establishes a solid foundation for maintaining control over the dynamic energy balance within the system.

The AHE and overall behavior of the reactor are determined by comparing the effects of various gases inside the reactor (vacuum, Ar, He, and He-Ar mixtures), serving as cross-checks and calibrations against the active gases H_2 or D_2. A key aspect of temperature measurement is monitoring the external reactor wall temperature, specifically at the point corresponding to the center of the internal coil. The thick glass tube containing the core is wrapped with two layers of thermally conductive and internally reflective thick aluminum foil.

Room temperature and humidity were kept as stable as possible using three air conditioners, and were measured for each data point (with these values subtracted from the reactor wall temperature). Even the wind speed around the reactor was monitored. The side of the aluminum foil facing the ambient environment was darkened with a special black paint, achieving about 95% emissivity.

Fortunately, in our experiments, the initial measurements using H_2 were similar to those with He, which serves as our primary reference. To gain a clearer understanding of the true temperature of the wire, we also measured the internal reactor temperature. For additional clarity, an example of the AHE determination is provided in the addendum.

1.1. Calibration Procedures & Observations

This section provides a comprehensive overview of key calibration procedures and observations integral to our experimental investigation. Anecdotal observations since 2011 have revealed a critical timeframe for achieving complete de-loading of Constantan from adsorbed Hydrogen or Deuterium—within the first 3-4 days from the experiment's initiation. Delayed de-loading beyond this period often leads to the persistence of residual H and D within the lattice, introducing unpredictability into subsequent calibrations.

Our primary calibration strategy used helium under DC conditions with negative polarity at pressures similar to those applied later with active gases, ranging from 0.5 to 2 bar (see Addendum A). Additional cross-calibrations were performed with vacuum, argon, and helium-argon mixtures to validate data consistency and align it with the expected behavior of dissipative systems in free air. Notably, experiments with argon-helium mixtures proved significant, as internal temperature increases were observed. This was attributed to argon's lower thermal conductivity, which enhances its insulating properties compared to helium. Temperature measurements were crucial and were conducted using K-type thermocouples. These thermocouples are notable for their external shielding made of stainless steel with a diameter of 1.5 mm. Internally, they are electrically insulated with magnesium oxide (MgO) powder, which enhances their precision and reliability. For AHE measurements, we specifically used the temperature at the reactor's external wall (T_{ext}), in open air. This method minimizes the risk of measurement errors from hydrogen potentially entering through the stainless steel sheath of the K-type thermocouple.

Measurements were taken both at the external wall of the robust glass reactor and within the core of the internal coil, as shown in Fig. 1 and Fig. 2, respectively. To protect the borosilicate glass surface of the reactor, two layers of reflective, thick aluminum foil were applied, along with a high-emissivity, thermally resistant paint capable of withstanding temperatures from -50 °C to 800 °C.

Figure 1 shows the schematic of the reactor body—a robust container specifically designed for high-temperature and mild-pressure experiments. Constructed from a borosilicate glass tube with a thick 3.2 mm wall and manufactured by "Vetreria Scientifica Spaziani-Italy," this design ensures both reliability and safety during high-temperature operations.

Figure 2 provides a detailed view of the reactor's inner core setup, featuring a coaxial coil and its inner iron (Fe) counter-electrode. Initially, the coil measured 158 cm in length with 75 turns, but it was later modified to 26 turns with a larger diameter to address issues with high-voltage insulation and the incorporation of powders into the glass fiber sheaths. Despite the differences, the lengths of both the 75-turn coil (without powder) and the 26-turn coil

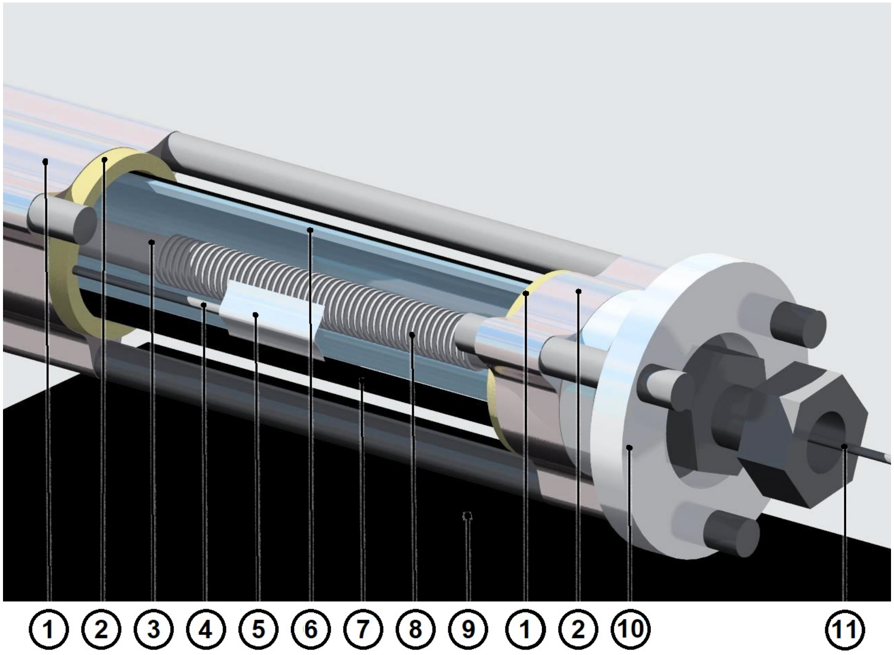

Figure 1. Reactor Body Schematic. This schematic illustrates the reactor body, a robust container specially designed and rigorously tested for high-temperature and mild-pressure experiments. The components are as follows:
1. Aluminum Reflecting Foil
2. Heat-Insulating Carpet (Aeropan Ca)
3. Counter Electrode
4. Stainless Steel Shielded "Type K" External Thermocouple
5. Aluminum Reflecting Foil and Thermal Insulating Carpet (Aeropan Ca) − Applied on the external thermocouple (4)
6. Borosilicate Glass: Length = 50 cm, external/internal diameter = 40/33.6 mm
7. Aluminum Reflecting Foil with Blackened Outer Side − Placed on the glass (6)
8. Coil
9. Aluminum Plate with Blackened Top Side
10. Stainless Steel Frame
11. Stainless Steel Covered "Type K" Internal Thermocouple

(with powder-filled sheaths) are quite similar, each approximately 150 cm in length. This setup, depicted in Fig. 2, demonstrates how the coil diameter significantly increases when the glass sheaths are filled with powders.

Figure 3 provides an overview of the internal reactor temperature, expressed as the temperature difference (ΔT) between the internal temperature (T_{int}) and the ambient temperature (T_a). ΔT is shown as a function of the input power (P_{in}), which ranges from 5 to 170 W using direct current (DC). Additionally, the figure illustrates the ratio of ($T_{ext} - T_a$) to P_{in}, offering further insights into the reactor's thermal behavior under different power levels.

The findings indicate that as the thermal conductivity of the gases decreases, the internal temperature rises, with the highest temperature observed in a vacuum. The difference in input power required to maintain a specific wall temperature (T_{ext}) between helium and other gases is referred to as ΔW. Figure 4 summarizes key observations from the DC experiments, showing the impact of H_2 and a 50:50 H_2-Ar mixture on both internal and external temperatures. Notably, ΔW varies between the initial hydrogen run (H_2#1) and a later run (H_2#4). This variation cannot be explained

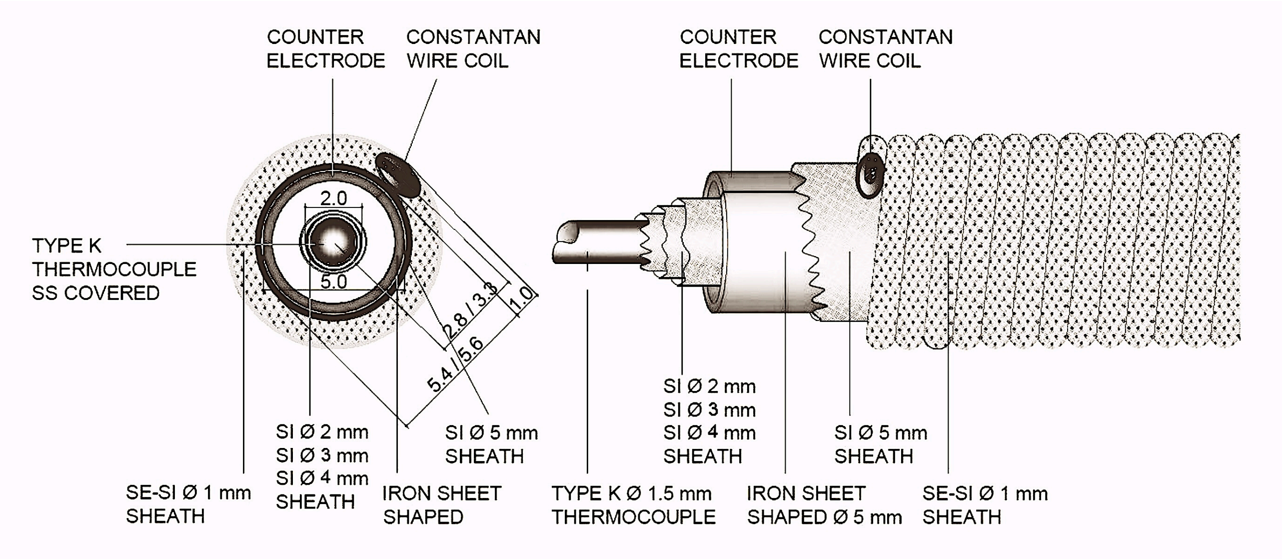

Figure 2. Reactor Inner Core Details of the standard/simplified set-up, used for both pulsing tests and to prevent unexpected interferences from Cu tapes and SS tube, as seen in the previous setup.

by conventional heat transfer mechanisms alone but is attributed to Anomalous Heat Effects (AHE). Importantly, under DC conditions, the coil remains at a negative voltage relative to the counter electrode throughout the experiment.

Figure 4 shows change in power (ΔW) values, normalized to helium (He), along with the corresponding internal temperature trends. The data were obtained from experiments using pure hydrogen (H_2) (experiments #1 and #4), an argon-helium mixture (Ar-He, 55:45 by volume), and a hydrogen-argon mixture (H_2-Ar, 50:50 by volume). Notably, ΔW observed with H_2 increased from experiment #1 to experiment #4, indicating the presence of Anomalous Heat Effects (AHE). The negative ΔW values during the H_2#1 experiment at low power may result from increased heat losses in hydrogen compared to helium (see Addendum A). At input powers above 120 W, AHE may begin to manifest at temperatures above 500 °C.

The negative ΔW values with the argon-helium mixture (Ar-He) could be attributed to greater radiative losses due to the higher internal temperature. The "positive aging" procedure, which involves maintaining the wire at the highest power level for an extended period (24–96 hours), is influenced by the combined effects of H_2 pressure, elevated temperatures, and significant electromigration voltage and current. In the figure, the reactor's internal temperature is shown by bluish lines, while ΔW values are represented by red-orange lines.

It's important to note that normalizing AHE to helium (He) implies that AHE is considered zero when helium is the operating gas. The temperature increase observed under the H_2-Ar mixture is attributed to a potential abrupt absorption of hydrogen within the reactor. This absorption likely alters the H_2/Ar ratio, leading to significant changes in the internal temperature.

Figure 5 illustrates the oscillation power circuitry used to generate controlled amplitude oscillations from the mains (220 Vac, 50 Hz), with voltage adjustments enabled via a Variac. The output is galvanically isolated from the reactor by a standard laminated iron-core transformer, ensuring safe operation. Both the Variac and transformer preserve the sinusoidal waveform of the 50 Hz mains voltage, modifying only its amplitude to match the requirements of the wire,

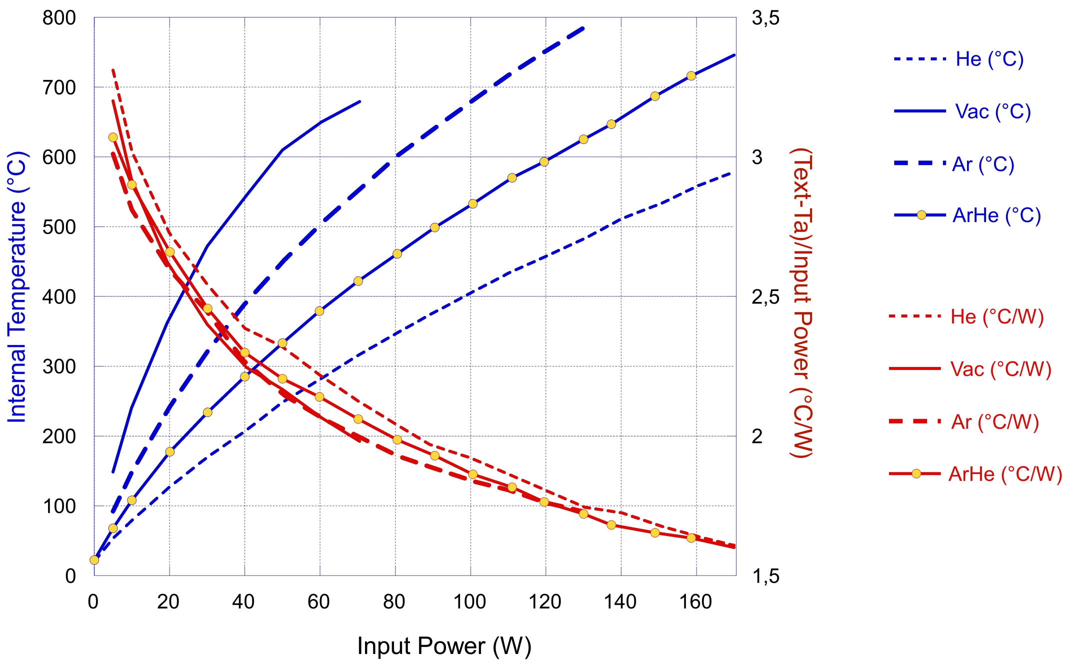

Figure 3. Calibration in DC: This figure provides a comprehensive overview of the reactor internal temperature (T_{int}, left axis) and the ratio of the temperature difference (ΔT) between the external reactor temperature and ambient temperature ($T_{ext} - T_a$) relative to input power (P_{in}, right axis). Input power levels vary from 5 to 170 W, as operationally feasible. For safety reasons, maximum temperatures were capped around 800 °C. The experiments were conducted under varying gas pressures—generally a few bars—using helium (He), argon (Ar), and a 55:45 volume mixture of argon and helium (Ar-He), in addition to vacuum conditions.

which typically has a resistance of approximately 22–30 Ohms following chemical and physical treatments, excluding hydrogen absorption. Notably, the wire's resistance drops significantly during substantial hydrogen (H) loading.

This figure shows waveform shapes of Sinusoidal Symmetric (SS), Unipolar Positive (UP), and Unipolar Negative (UN). Figure 6 presents a typical Unipolar Negative pulse waveform, highlighting some mild deviations and irregularities from the ideal pure sinusoid at 50 Hz, due to distortions caused by the Variac, decoupling transformer, and power diode. The power signal, shown in green, is able to capture even these minor irregularities thanks to the large bandwidth of the oscilloscope (100 MHz).

For the purpose of this figure, the Constantan coil is modeled as an ideal inductor in series with a 24 Ohm resistor, as shown in the figure. The 24–26 Ohm range is characteristic when the wire is under hydrogen loading and subjected to current. Additionally, a detailed characterization of the circuit's voltages and currents during the various stimulation modes is provided in Addendum B.

Figure 6 shows a snapshot of the oscilloscope screen.

Figure 7 provides a comprehensive comparison of AHE normalized to helium runs, demonstrating the effects of different polarizations and pulse waveforms on AHE generation. The data confirm the effectiveness of unipolar negative pulse stimulation (UN) in enhancing AHE, as previously observed. Measurements conducted in pure H_2, combined with the beneficial effect of higher internal temperatures achieved by adding argon (Ar), offer a deeper understanding of the phenomena. The synergistic effect of introducing argon (Ar) and applying unipolar negative

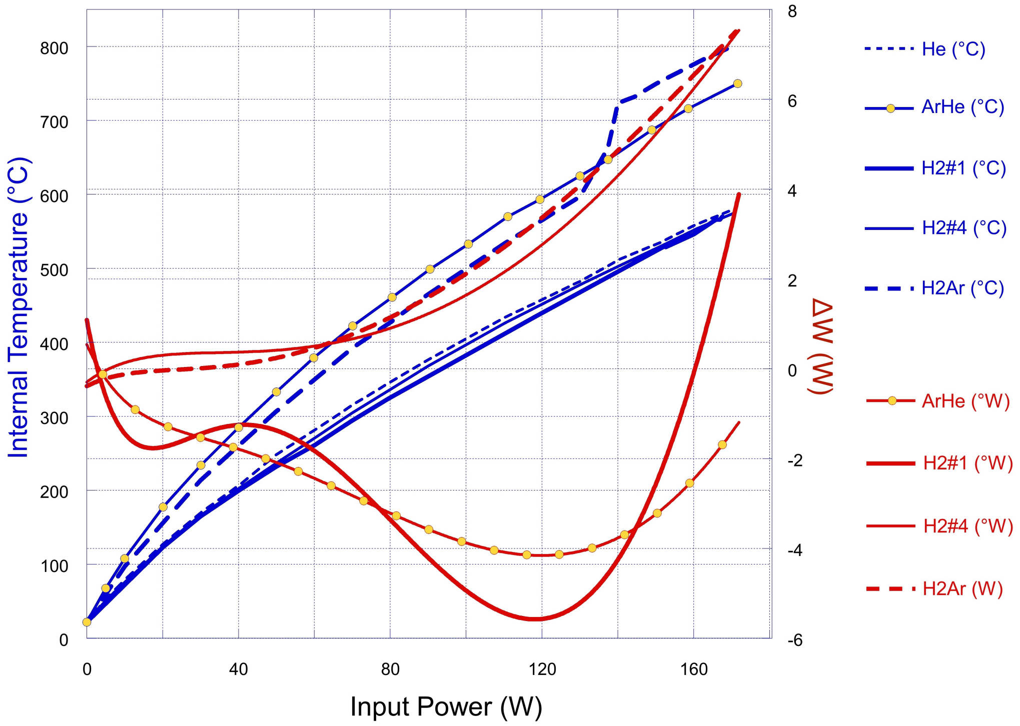

Figure 4. Experiments Using DC Currents. The change in power (ΔW) normalized to helium (He), along with the corresponding internal temperature trends.

pulses resulted in notable AHE values exceeding 23 W (at an input power of 170 W). This result is likely due to the near-grounded state of the counter-electrode, facilitated by a 10 MΩ resistor, which compensates for the intrinsic impedance of the multimeter.

2. Discussion

We believe that the reactor developed at INFN-LNF, despite its elementary construction and reliance on a thermometric energy balance, is sufficiently reliable for the intended experiments. Notably, the calibration results—including those for vacuum, argon (Ar), argon-helium (Ar-He), and helium (He)—align closely with theoretical expectations when the input power exceeds 20 W.

Comparative experiments with pure hydrogen (H_2) at lower internal temperatures versus argon-hydrogen (Ar-H_2) mixtures at higher temperatures have confirmed that increasing the internal temperature—beyond 500 °C, where Low Work Function materials start emitting electrons—leads to a measurable increase in Anomalous Heat Excess (AHE).

The observed enhancement in AHE, attributed to electron emissions and surface ionization, is assessed by monitoring the temperature of the external reactor wall, which serves as our primary reliable data for quantifying AHE (see addendum A for further details). This increase in AHE is sufficient to counterbalance the energy dissipation at

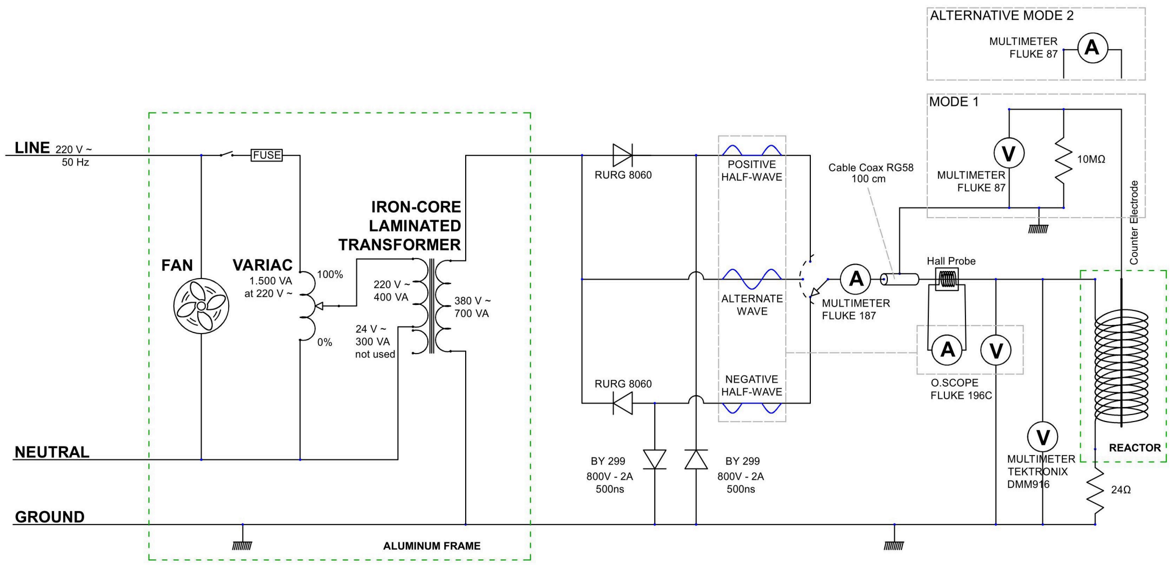

Figure 5. Oscillation Circuitry. This figure illustrates the circuitry designed to generate controlled amplitude oscillations from the mains (220 Vac, 50 Hz), with voltage adjustments enabled via a Variac.

the reactor's extremities, including the unmeasured temperatures of the flanges. Therefore, our AHE estimates are considered conservative, suggesting the potential for even more significant results.

We have observed that an appropriate "annealing-conditioning" procedure in hydrogen (H_2) has a substantial impact on increasing the value of Anomalous Heat Excess (AHE). This can be readily seen in Figure 4 when comparing the first and fourth runs in pure hydrogen (H_2#1 versus H_2#4). This conclusion is derived from straightforward experiments with pure H_2, where input power and temperature are gradually cycled up and down over several hours. Additionally, the wire is maintained at maximum temperature for extended periods (24–96 hours). This procedure results in a progressive increase in AHE with an increasing number of cycles and time, reaching near saturation under the given operational conditions, including internal temperature, gas pressure, current, and voltage.

Furthermore, our results reaffirm previous observations, as presented at ICCF24 and IWAHLM15, regarding the compatibility of our findings with the formation of hydrogen-enhanced Super Abundant Vacancies (SAV) due to prolonged electromigration along the wires.

Interestingly, this aligns with the insights of Professor M. Staker from Loyola University (USA), who emphasizes the role of Super Abundant Vacancies (SAV) [10], [11], [12]. Previously identified by Professor H. Fukai at Tokyo University, this phenomenon was observed in palladium (Pd) wires. Our hypothesis that the SAV effect plays a significant role is supported by the positive aging effects observed at high power levels and through multiple loading and unloading cycles, which align with Professor Staker's findings. Furthermore, in some of our previous experiments, we noted that when the reactor is left idle for extended periods (hours to days) without sufficient electromigration, it reverts to near-initial Anomalous Heat Excess (AHE) conditions, which are almost negligible. This suggests that the "active species" within the bulk and/or near the surface exists in a metastable state. Similar observations have been

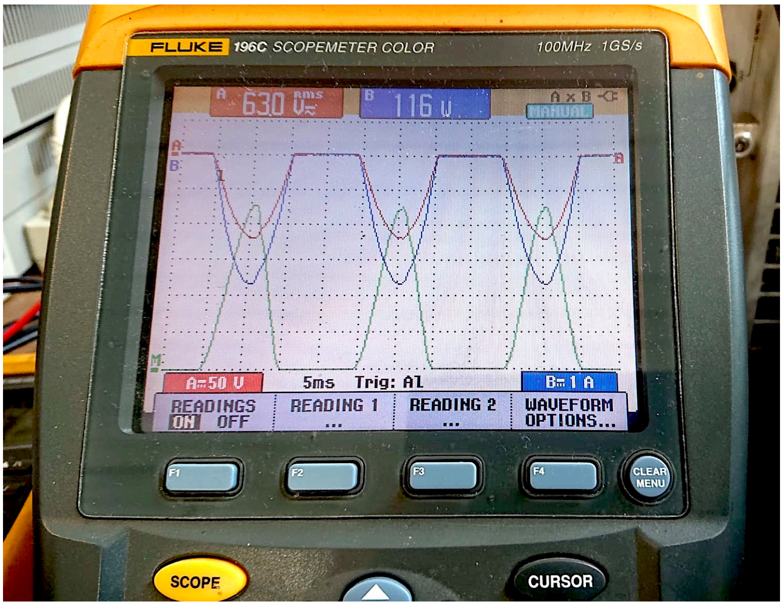

Figure 6. Oscilloscope Snapshot A representative oscilloscope snapshot captures the outcomes under 50 Hz unipolar negative excitation, with voltage represented in red, current in blue, and power in green.

made by our team with nickel and its alloys, including Constantan (Ni-Cu-Mn), though these findings have not yet been published.

Our results also confirm (as shown in Fig. 4) that hydrogen (H_2) is essential for generating AHE, even when mixed with argon (Ar). This is evident when comparing experiments using argon-helium (Ar-He, 55:45 by volume) versus argon-hydrogen (Ar-H_2, 50:50 by volume). Key experiments, shown in Figs. 7 and 8, involving argon-hydrogen mixtures at a pressure of 1 bar, reveal a significant dependence of AHE on the power supply waveform.

We have observed that, at the same input power, alternating current (AC) results in increased Anomalous Heat Excess (AHE) compared to direct current (DC), as indicated by the curve. Note that unipolar positive (UNP) and unipolar negative (UN) pulsed conditions are both types of AC. This outcome is likely due to the higher voltage (and current) values at the peaks of the AC waveform. For a pure sinusoidal waveform, the peak voltage is approximately 1.41 times larger than its root mean square (RMS) value. In the case of a unipolar-pulsed power supply, this effect is further amplified because the effective duty cycle is 50%, meaning the intrinsic energetic content during the active phase of the pulse is effectively doubled compared to DC.

Interestingly, the beneficial effect of pulsing is predominantly observed with negative polarity (UN), while positive polarity (UP) closely resembles DC conditions. Additionally, the symmetric sinusoidal (SS) waveform produces AHE results that fall between those of UN and UP, reinforcing the nature of these effects.

The exact reason for the enhanced AHE observed with negative pulses remains unclear. However, it is worth considering that unipolar pulses increase the total peak voltage, which significantly raises the ΔV/cm parameter (voltage drop per unit length) that governs electromigration. The differing effects of positive versus negative voltages relative to the counter electrode deserve further investigation. In the case of unipolar pulses, the lower measured voltage values (compared to negative pulses) combined with an equivalent increase in current suggest additional hydrogen loading within the bulk of the Constantan wire, driven by the negative voltage.

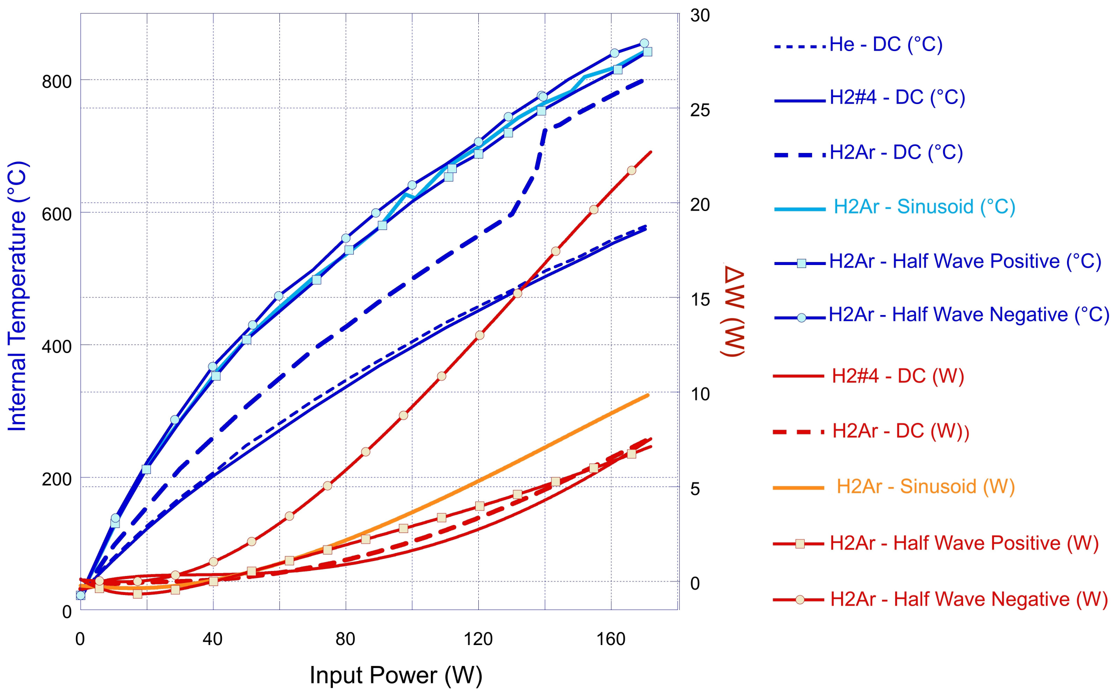

Figure 7. AHE Comparison. This figure provides an analysis of Anomalous Heat Excess (AHE), illustrated by ΔW values under varying current types, including both direct current (DC) and alternating current (AC) with different waveform profiles. Internal reactor temperature trends are shown in blue-toned lines, while ΔW (indicative of AHE) is marked by red-orange lines. This visualization underscores the influence of waveform characteristics on AHE, with a particularly pronounced AHE response for the Half-Wave Negative current, suggesting a potential optimization route for maximizing excess heat under specific conditions.

As extensively reported for Constantan since the late eighties, based on research at Dresden University in Germany [13], hydrogen loading reduces the material's resistivity. We have consistently observed this effect since 2011, and it proves to be highly reproducible.

Consistent with our earlier observations, unipolar negative pulses continue to yield the most favorable values of Anomalous Heat Excess (AHE). This trend aligns with our previous studies dating back to 1994 [14], [15], where we investigated palladium (Pd) wires and applied negative High Peak Power Pulses (HPPP) with durations typically ranging from a few microseconds (μs) and repetition rates up to 30 kHz. In our recent experiments with Constantan, the pulse duration averaged around 10 μs, with a repetition rate between 1 and 2.5 kHz, as documented in the ICCF23 Proceedings [3].

Although there are significant differences between the setups used in the 1990s with electrolytic systems and those used today, it is important to recognize the origins of our impulse approach and its evolution over time, as documented in our team's publications.

Importantly, within the parameters of our ongoing experiments, the comparison of Anomalous Heat Effect (AHE) values obtained through positive and negative pulses serves as compelling evidence, effectively refuting the possibility of errors in AHE estimation stemming from thermometry inaccuracies or misconceptions about input energy.

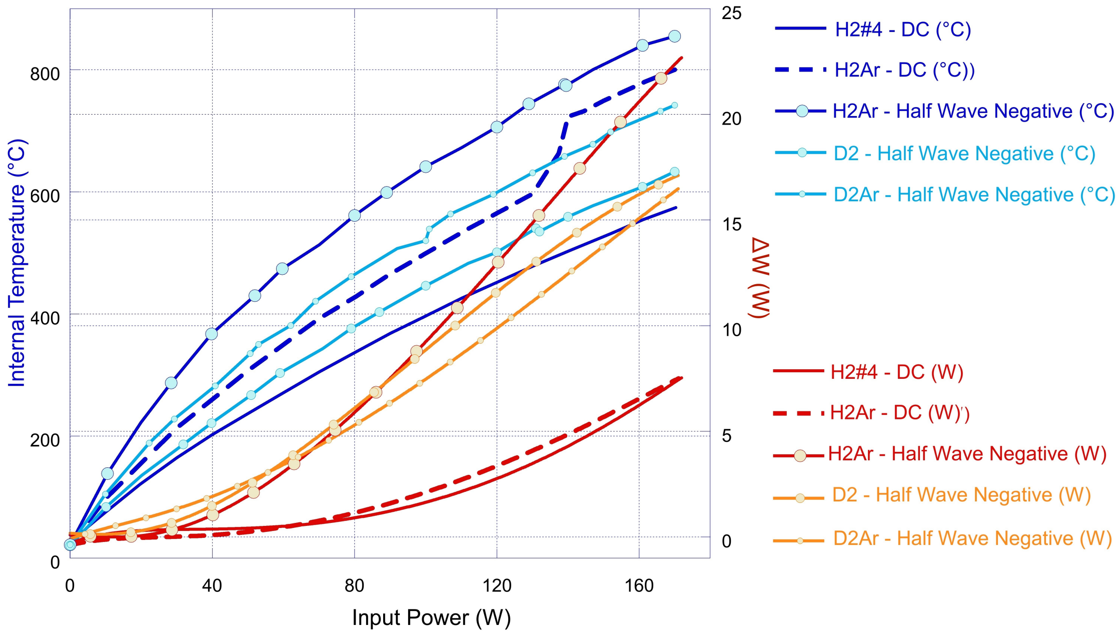

Figure 8. Key experiments using argon-hydrogen (Ar-H_2) and argon-deuterium (Ar-D_2) mixtures at a pressure of 1 bar reveal a marked relationship between ΔW (or Anomalous Heat Excess, AHE) and the waveform of the applied power. Findings show that, with equivalent input power, alternating current (AC) half-waves consistently produce higher AHE values compared to direct current (DC), suggesting that waveform modulation plays a critical role in enhancing excess heat generation.

This conclusion is supported by meticulous measurements conducted using the 100 MHz digital oscilloscope in the current experimental setup.

Subsequent to the ANV11 Workshop in December 2022 and preceding the ANV12 presentation, we conducted experiments explicitly designed to investigate the effects of possible 'deliberate damages' to the specific active section of the wire, such as the Super Abundant Vacancies (SAV) volume. This involved the introduction of 1 cc of water in the reactor and heating the wire to internal temperatures of up to 550 °C over an 18-hour period, followed by vacuum degassing at elevated temperatures reaching up to 580 °C over approximately 4 hours in total. For the sake of expediency, subsequent experiments were conducted exclusively with pure deuterium (D_2) and D_2-argon (D_2-Ar) mixtures, utilizing unipolar negative pulses. These experiments are summarized in Fig. 9, which provides a comprehensive overview of a specific experiment designed to scrutinize the impact of severe gas changes and prolonged vacuum treatments at elevated temperatures on Anomalous Heat Effects (AHE). The primary objective of this experiment was to investigate the suppressive effects of injecting water into the reactor on AHE. For the sake of simplicity, we employed solely pure D_2 (pure deuterium) and a D_2-Ar mixture in a 50:50 ratio, combining deuterium with argon. Following the injection of water, a discernible reduction in AHE was observed compared to the preceding "pristine" H_2-Ar 50:50 conditions, indicating that the introduction of water had a suppressive effect on AHE. Interestingly, the inclusion of argon (Ar) alongside deuterium (D_2) exhibited limited effects on AHE, at least after a 10-day "recovery time," as suggested by the experimental observations.

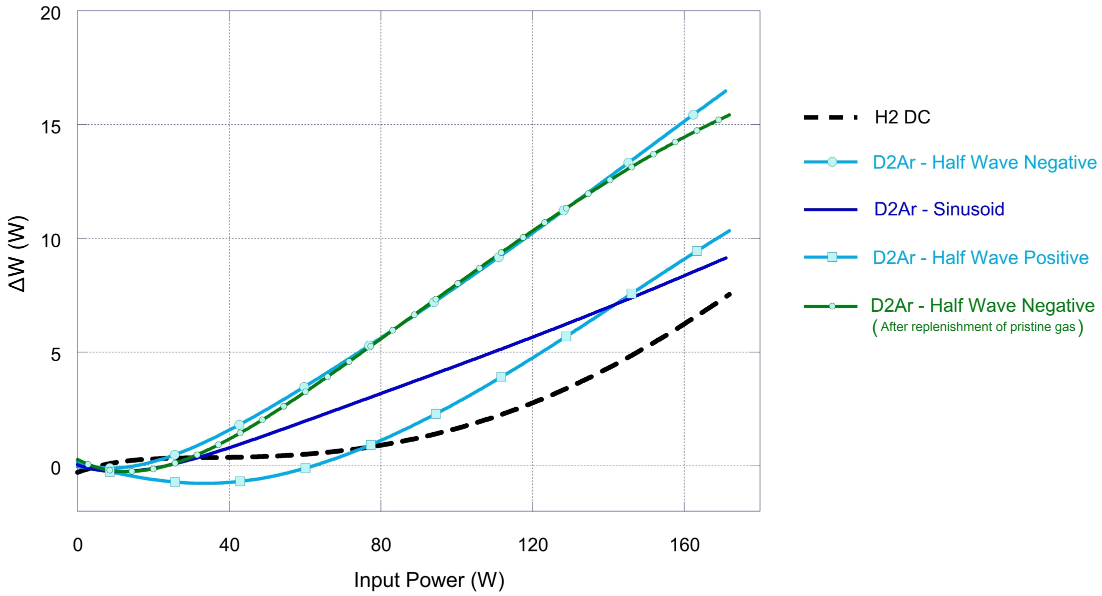

Figure 9. A comparative analysis of Anomalous Heat Excess (AHE), expressed as ΔW, was performed using the same initial gas mixture (D_2-Ar, 50:50 by volume) under various excitation modes: Negative Half Wave UN1, Positive Half Wave UP1, Sinusoidal Wave SS1, and a subsequent Negative Half Wave UN2. Notably, in the second UN2 run—conducted after refilling with D_2—AHE values were slightly lower in the higher power ranges. This observed reduction in AHE is likely due to the adverse effects of prior water treatments, which may have impacted the material properties or gas-phase interactions within the reactor.

2.1. Further Experiments to Confirm the Role of Negative Pulsing

To thoroughly assess the significance of pulsing polarity on Anomalous Heat Excess (AHE), a series of dedicated experiments was conducted, beginning January 23, 2023, using an Ar-D_2 (50:50) gas mixture. The goal was to evaluate the reliability of the procedure and identify potential errors in the context of SAV structures that had undergone previous damage, including water addition and extended degassing at high temperatures.

In total, five experiments were carried out, consistently using the same initial gas mixture (Ar-D_2, 50:50 by volume) with an initial pressure of approximately 2.3 bar at room temperature. The sequence of stimulations and their respective data were as follows:

a) **UN (Unipolar Negative Stimulation, UN1, January 24-26, 2023):** A full cycle with power levels of 170 W, 10 W, and 0 W.
b) **UP (Unipolar Positive Stimulation, UP1, January 26-31, 2023):** A full cycle with power levels of 170 W, 10 W, and 0 W.
c) **SS (Sinusoidal Stimulation, SS1, February 1-6, 2023):** A full cycle with power levels of 170 W, 10 W, and 0 W.
d) **UN (Unipolar Negative Stimulation, UN2, February 6-13, 2023):** A full cycle with power levels of 170 W, 10 W, and 0 W.
e) **UN (Unipolar Negative Stimulation, UN3, February 14, 2023):** A single measurement at 144 W.

The AHE curves for each experiment are shown in Fig. 9, constructed from multiple intermediate power measurements taken in 10 W increments, ranging from 10 W to a maximum of 170 W. The experimental outcomes closely mirrored those shown in Fig. 8, further confirming the influence of pulse polarities on AHE behavior. For clarity and simplicity, additional figures have been omitted.

2.2. In-Depth Analysis

The results with the D_2-Ar mixture (50:50 by volume) were qualitatively similar to those obtained using the previous H_2-Ar (50:50 by volume) mixture, as shown in Fig. 8. In both cases, the Anomalous Heat Excess (AHE) values followed the same trend: UN > SS > UP across most power regimes. However, some reduction in AHE performance was observed due to prior "damaging procedures."

An intriguing possibility is that the D_2-Ar mixture may perform less effectively under pulsed conditions compared to H_2-Ar, suggesting a reverse isotopic effect relative to what was previously observed under direct current (DC) conditions. This could be due to deuterium (D), being heavier than hydrogen (H), facing more challenges in "moving" within the metal lattice under pulsed stimulation.

"Experiment d" displayed almost identical behavior to "Experiment a," highlighting the reproducibility of the phenomena, even after a significant pressure reduction. Both external and internal temperatures increased, which were critical for energy evaluations, confirming that the source of AHE is internal to the reactor core.

Remarkably, no performance decline was observed during long-term pulsed operations. In fact, during continuous operation over extended periods (over 60 hours, including weekends), the AHE was greater than during the typical 60–90 minutes of excitation at fixed power.

Following "Experiment e," the wire fractured due to an incident involving the development of new electrical stimulation methods. This occurred with the inaugural version of the dimmer, featuring a Triac in its final stage. The fracture is believed to have been caused by excessive electrical power input, exceeding 1500 W.

3. Experiments Using Virgin Wires

Two experiments were conducted using Constantan wires without any physical-chemical treatments before placing them inside the reactor. These wires had the typical dimensions (length $l = 158$ cm, diameter $\Phi = 200$ μm) and resistance R = 25 Ohm.

Experiment #1: The experiment commenced on February 27, 2023, and was abruptly concluded on March 27, 2023. Due to various external factors, only detailed calibrations were performed during this period. Despite the qualitative nature of these calibrations, the results were consistent with previous experiments using "treated" wires. However, when H_2 was introduced for the first time, the wire experienced catastrophic failure.

Our experience suggests that untreated wires are more prone to breaking than treated ones. This observation is particularly relevant given that the chemical treatments involved applying a coating using a water solution of nitrates. We speculate that a small amount of hydrogen may have been absorbed into the wire from the water. However, we do not yet have direct evidence of this absorption. This hypothesis has been a longstanding consideration and will be a focus of future investigation.

Experiment #2: Began on 29 March 2023 and concluded on 17 July 2023, once again due to catastrophic failure. The calibrations for experiment #2 closely resembled those of experiment #1. After introducing H_2, which occurred 8 days into the experiment, the results were qualitatively similar to those of the treated wires typically used. The main differences observed were a lower intensity of AHE and, overall, greater instability of AHE. At times, this instability even led to "negative" values of AHE (relative to the standardized He calibration), similar to what was observed in loading #1 (Fig. 4), as presented during the ANV12 Workshop.

However, when we applied longitudinal unipolar pulses with an input power of 170 W, 16 days after the experiment's commencement (using a unipolar negative shape), the Anomalous Heat Excess (AHE) briefly surged to 5.5 W. Unfortunately, this increase was short-lived, and the AHE soon dropped to values closely resembling those observed during the helium calibration.

We attempted several approaches to recover the initially observed AHE without success. These included prolonged application of longitudinal pulsed conditions and the application of a transverse electric field. The transverse field was applied using a counter electrode and a low-power transformer with a nominal gain of 2, sourced from a 50 Hz AC line (230 Vac, approximately $\pm$320 V peak). The AC field was applied symmetrically and unipolarly at $\pm$600 V, while DC conditions were tested up to $\pm$1000 V with currents ranging from 0.1 to 5 mA.

In general, the AHE obtained from untreated wires was lower than that from treated wires, and the positive effects of aging under Hydrogen and/or Deuterium were negligible. Furthermore, the stability of AHE over time was poor. The wire suffered catastrophic failure during a test involving Deuterium and bipolar pulses at approximately 170 W of input power, the typical maximum value applied in our experiments. Based on the unsatisfactory results obtained, we are nearly convinced that some form of chemical-physical pre-treatment of Constantan wires is absolutely necessary to achieve reliable and repeatable results in terms of AHE generation. In other words, high-power pulsing, at least under our present "gentle" operating conditions at 50 Hz, yields some positive effects with respect to AHE, but these effects are not stable over time. Therefore, it appears that there is another co-factor that plays a crucial role in achieving consistent results.

4. Procedures to Reduce Power Losses During the Generation of Pulses to Activate AHE

MOTIVATION: In the study of Anomalous Heat Excess (AHE) effects, a crucial yet often overlooked parameter is the energy "wasted" in generating the required waveform during electromagnetic excitation. Typically, AHE observations focus on the final section of the reactor, but it's important to consider the energy efficiency of the equipment used to generate the waveform.

For direct current (DC) power supplies, conventional generators have an electrical efficiency of approximately 50%. This efficiency can improve to 80–85% when using switching-mode AC-DC converters, though these may introduce high-frequency noise (20–100 kHz) that can cause unforeseen issues. The efficiency of power transfer drops significantly in high-power pulsing applications, often falling to around 30% due to the complexity of the circuitry involved.

To provide a comparative perspective, consider the example of Hot Fusion by Laser, as demonstrated by the National Ignition Facility (NIF) in the USA on December 5, 2022. The experiment utilized 192 lasers, consuming a staggering 322 MJ of input energy. After wavelength conversion, these lasers produced approximately 2.10 MJ of "useful" ultraviolet (UV) light over a duration of about 1 nanosecond, which was directed at a Deuterium-Tritium pellet. Following compression and implosion, the total energy emitted in the form of nuclear radiation amounted to about 3.15 MJ. This resulted in a net gain of 1.05 MJ, representing a "local gain" of approximately 50%. However, when considering the total energy balance, it becomes clear that 320.95 MJ of energy was lost in the process, from laser excitation to nuclear particle emission. Furthermore, these calculations do not account for converting this "nuclear radiation" into usable energy forms, such as by harnessing it to generate steam for power production.

5. INFN-LNF General Approaches and Their Motivation

Historically, our procedures have been developed over several years, starting in 1994 with the use of Pd wires [1], [2], [14], [15]. During this time, we found that negative High-Peak-Power-Pulses (HPPP) were capable of stimulating the production of Anomalous Heat Excess (AHE) and maintaining it for extended periods, sometimes up to a few days, especially in electrolytic environments [1], [2], [14]. However, there were limitations to this approach, such as being able to investigate only the effects of negative polarity and not positive or bipolar pulses. The construction of pulses was complex, and coupling with the low-impedance reactor required special ancillary devices, including multiple parallel coaxial cables. This time around, we decided to adopt a different strategy: We chose to utilize "standard" commercially available circuitry and instrumentation that could be easily connected directly to the 230 Vac, 50 Hz power line, specifically Line (L) and Neutral (N), in accordance with the regulations in Italy. The auxiliary circuitries, which are crafted in-house, must prioritize simplicity. The plan was to routinely test with waveforms of different types, including sinusoidal bipolar, only positive, and only negative. We kept the circuitry relatively simple to avoid potential side effects from the 50 Hz line connected to the reactor core, which was arranged as several turns of a coil wound around magnetic material (Fe). Regarding power variation: to match the 230 Vac line with the reactor's resistance (around 25–30 Ohms, wire diameter 200 μm) and accommodate operational constraints (such as keeping the internal temperature below 800 °C and power below 180 W), we chose a straightforward approach. We used a Variac, which is a voltage-variable auto-transformer, and placed a voltage transformer in series to provide galvanic insulation between the 50 Hz–230 Vac line and the reactor body. The external side of coaxial connectors was grounded for safety reasons.

6. Energy Loss Reduction and Performance Improvements

The setup illustrated in Fig. 5 met the majority of our operational requirements, particularly the ability to generate unipolar pulses. This was achieved by incorporating fast, high-current diodes with minimal voltage drop into the system. However, overall energy loss remained relatively high. For instance, at an injected power of 170 W—the maximum input power for our standard experimental configuration, which employs a 158 cm length of Constantan wire with a 200 μm diameter—the energy losses totaled approximately 70 W. This figure excludes the additional 14 W required by the fan cooler, a necessary component to prevent overheating of the Variac and transformer copper wires due to the flowing current ($P_{in} = I^2R$). As temperatures increase, resistance rises, leading to even greater energy losses throughout the system.

To improve system performance and reduce energy losses, we introduced a high-efficiency toroidal transformer with an output power optimized for our specific power range, as shown in Fig. 10.

Innovative Use of Dimmer for Energy Efficiency

To address challenges with energy losses, we adopted an unconventional solution in our LENR studies: a commercial "Dimmer" originally designed for adjusting the brightness of tungsten incandescent lamps. Standard dimmers typically handle up to 150 W, with specialized models supporting up to 350 W. However, these devices have limitations in their dynamic range and require additional circuitry for specific needs like unipolar pulsing in our experiments.

After an incident on February 13 with a "standard" dimmer—featuring a single Triac for power control and less-than-optimal efficiency for unipolar pulses, which require additional energy-absorbing components—we decided to upgrade to a more capable model. The chosen unit offers a significantly higher power rating, up to 2300 VA, and features two independent high-power Silicon Controlled Rectifiers (SCRs) in the final stage for robust performance. We selected the TE8034 model from TECNEL-Italy, shown in Figure 11, for its superior handling capacity and reliability, making it an ideal choice for our experimental setup.

Figure 11 shows power control system configuration, which utilizes a high-power dimmer rated at 2.3 kVA (230 Vac). In this setup, the neutral (N) of the power supply is securely connected to ground (GND) through a stabilization circuit comprising two back-to-back 10 V Zener diodes, a 1 kΩ resistor, and a 2.2 μF ceramic capacitor. This arrangement ensures a stable reference point for oscilloscope measurements, benefiting from the typically limited fluctuation of the power supply's neutral, which generally remains within $\pm$1 V.

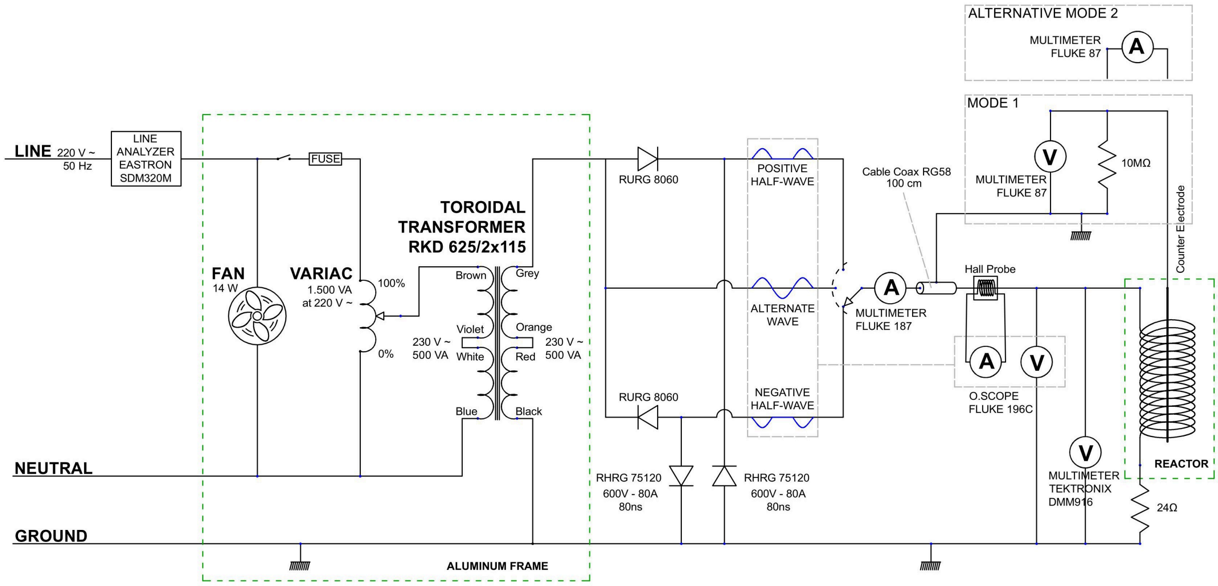

Figure 10. Configuration of the toroidal transformer, which closely resembles the thin-sheet iron transformer setup (as shown in Fig. 5). The primary distinctions are reduced weight and improved energy transfer efficiency. However, the fan cooler remains essential to mitigate copper coil resistance. The total losses, at an input power of 170 W, amounted to 30–35 W, excluding the fan's contribution.

In the "NETWORK SHAPER" circuitry, we adjusted the placement of high-power diodes (RURG 8060 and RHRG 75120) from their previous positions shown in Figures 5 and 10. This reconfiguration optimizes the speed and responsiveness of the Power Dimmer circuitry, yielding a voltage rise time of less than 1 μs under our specified conditions, thus enhancing overall system performance.

7. Conclusions, Next Steps, and Final Remarks

Despite the hypothesis presented in Section 2, the exact mechanisms behind the remarkable effects of pulsed currents on Anomalous Heat Excess (AHE) remain elusive. Nonetheless, several contributing factors can be speculated upon. Under pulsed current conditions, critical mechanisms include localized Joule heating, thermal fatigue, electromigration, and mechanical deformation. These processes can lead to localized densification and void formation, altering the density of the wire, particularly in regions exposed to high thermal or current stresses.

Periodic changes in wire density, along with impulsive electron emission and surface ionization, may drive the flux of atomic hydrogen within the metal lattice, potentially influencing AHE. Moving forward, we intend to combine the stimuli explored in this paper with pulsed dielectric barrier discharges (DBD), which were the focus of our 2018-2019 experimental campaigns [7]. This integration may offer deeper insights into the underlying phenomena that contribute to AHE.

Our research endeavors stand on the shoulders of numerous dedicated researchers and colleagues who, over the past three decades, have extensively explored the field of electric stimulation for low-energy nuclear reactions (LENR) and/or devised innovative configurations for active electrodes. Special recognition is owed to Thomas Claytor

FUSE Fast 10A	SDM320M - EASTRON NETWORK ANALYSER Active power (W) Voltage (V) Current (A) Frequency (Hz) Power factor (PF)	A9D17210 - SCHNEIDER MAGNETO-THERMAL DIFFERENTIAL 2-Pole Magneto-Thermal circuit breaker 10A Curve C 230V ~ 50Hz Differential 30mA Type A Acti9 IC60 RCBO	TE8034 - TECNEL SINGLE-PHASE VOLTAGE REGULATOR 2.3 kVA / 230V N.B. To be used only in configuration: line - neutral
DMM 916 - TEKTRONIK MULTIMETER Amperometer (A) Voltmeter (V)	PR30 - LEM HEME PROBE Amperometer (A) Hall effect 100 KHz	VP210 - FLUKE PROBE Voltmeter (V) 100 MHz	196C - FLUKE 2 Ch Oscillosc ophe Voltage (V) Current (A) Power (W) Time (s) 100 MHz

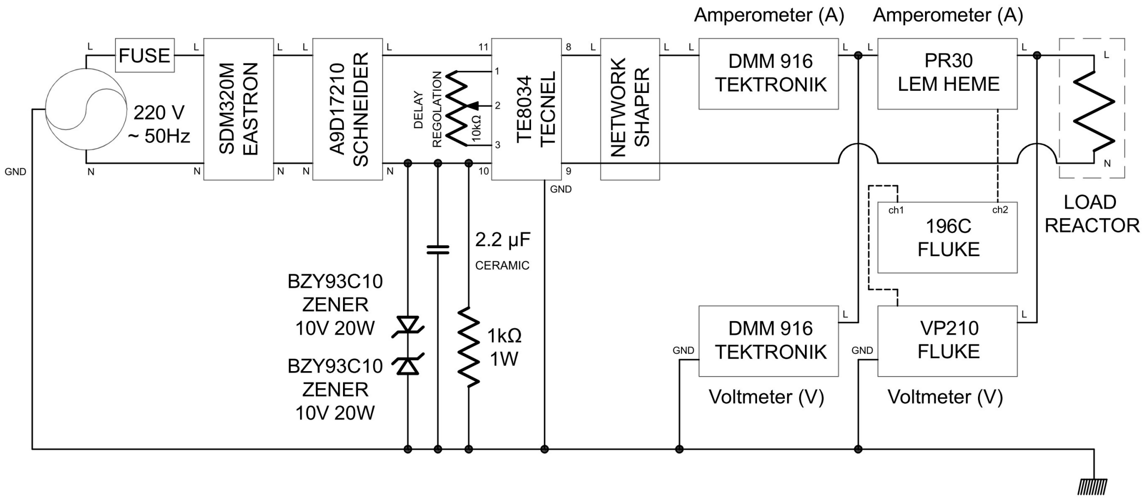

Figure 11. The power control system configuration, which utilizes a high-power dimmer rated at 2.3 kVA (230 Vac).

[16], [17], [18], [19], Jacques Dufour [20], [21], and Yasuhiro Iwamura [22], [23], [24] for their seminal contributions, and parallels can be drawn with the works of Thomas Passell [25] and Randell Mills [26], [27], [21]. Additionally, we are delighted by the recent findings presented by Dimiter Alexandrov [28], [29]. We interpret these results as a significant validation of our work, particularly in relation to Constantan wires.

In the pursuit of advancing low-energy nuclear reactions with anomalous heat effects (AHE), our latest efforts have yielded substantial progress in both circuitry innovation and the establishment of robust safety protocols.

The newly implemented dimmer-based circuit marks a significant advancement, not only in its successful assembly but also in achieving safety approval from the Electrical Installation Department of INFN-LNF, under the careful supervision of Ing. Ruggero Ricci. It is important to highlight that the operation of this system, particularly during the initial setup phases, requires the expertise of highly trained personnel to ensure safe and effective use.

A key qualitative difference in peak voltage modulation has been observed between the traditional Variac and the delayed phase conduction unique to the dimmer, as depicted in Fig. 13. Furthermore, a novel Constantan wire, which features a "mild coating" designed as an intermediate layer between heavy-coated and uncoated (virgin) wires, has

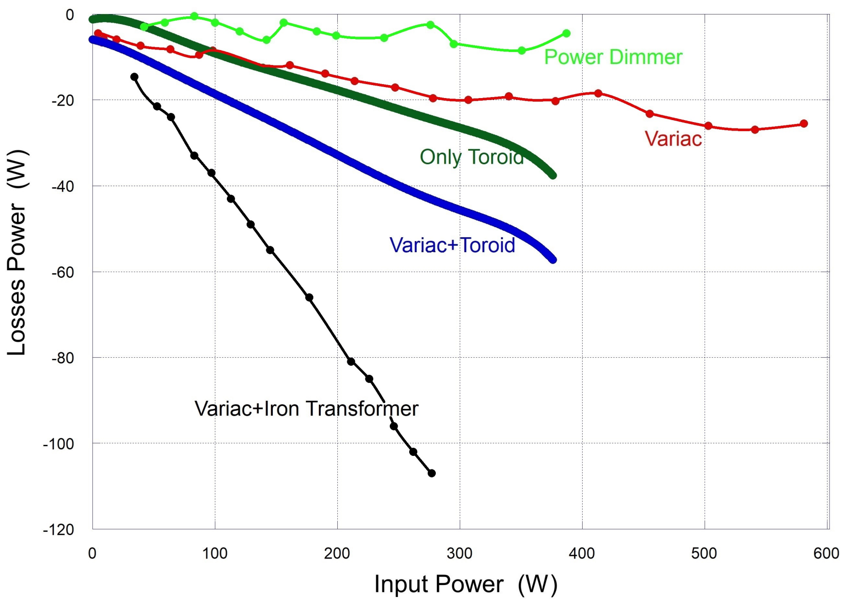

Figure 12. Comparison of power losses relative to input power among various configurations reveals distinct efficiencies: (a) the Conventional Variac with a laminated iron transformer has an approximate power loss of 75 W at 170 W input, (b) the Variac with a toroidal transformer reduces losses to about 35 W at the same input, and (c) the Power Dimmer configuration offers the lowest loss, ranging from 5 to 7 W at 170 W input. Notably, the Variac-transformer setups require an additional 14 W for fan cooling to manage heat buildup. The benefits of the Power Dimmer setup are clearly demonstrated, achieving the highest observed Anomalous Heat Effect (AHE) in our experiments, yielding between 23–25 W.

undergone extensive testing. The results have shown qualitative similarities to those presented at ≪ANV12≫, as well as to experiments conducted with virgin wires, demonstrating consistent performance across different wire treatments.

Initial tests using the power-dimmer circuitry under helium (He) and argon-helium (Ar-He) conditions did not reveal anomalous heat effects (AHE). Nevertheless, power losses were identified in sections without external temperature monitoring. Further refinements are deemed essential, highlighted by consistently lower $\Delta T/P_{in}$ values compared to direct current (DC) conditions.

Hydrogen (H_2) introduction resulted in "slightly negative" AHE results, reminiscent of the H_2#1 experiment presented at ANV12. Subsequent experiments involving pulsed conditions after H_2 absorption indicated a reduction in the R/Ro value, suggesting hydrogen absorption within the wire.

Post-ICCF25, our forthcoming plans include the comprehensive assessment of the power dimmer's stimulation of Anomalous Heat Effects (AHE), with the intent of presenting a comparative analysis with prior experiments conducted using the Variac. Additionally, we are committed to further exploration of phenomena associated with Super Abundant Vacancies (SAV). Expect updates and findings to be reported in the near future. The efficiency proof lies in the potential of the mildly treated wire to exhibit greater AHE under pulsed conditions than DC, signaling the efficacy of the procedure. This, in turn, serves as a foundational step for designing new core geometries and exploring chemical-physical treatments to enhance the Coefficient of Performance (CoP), bringing us closer to practical applications of LENR-AHE.

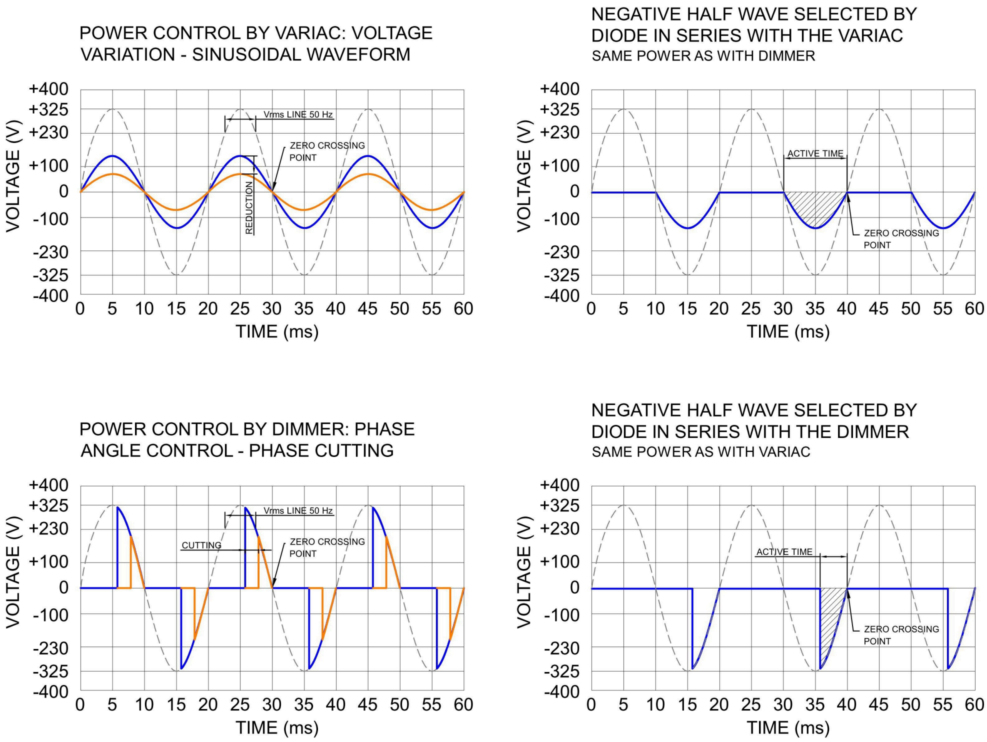

Figure 13. A comparative analysis of power control methods emphasizes the distinction in power control between: a) Peak voltage reduction through the use of a Variac, leading to substantial dissipation. b) Power Dimmer with phase angle control, which minimizes dissipation. In both scenarios, the inclusion of power diodes facilitates the generation of unipolar pulses.

Acknowledgments

We extend our sincere appreciation to the Metallurgical Company in North-Eastern Italy for their financial support and dedication to experiments that have been instrumental in independently verifying our key findings. Our partnerships with organizations such as SIGI-Favier, the CleanHME European project, Uppsala University in Sweden, and Broadbit Company have been greatly enriched by the outstanding contributions of scientists and researchers involved. We are particularly grateful to Dr. Augusto Marcelli at INFN-LNF for his invaluable scientific insights and solutions to challenges faced in the EU-INFN collaboration.

We extend our heartfelt gratitude to Prof. Mike Staker, the electrotechnical group at INFN-LNF, Engineer Ruggero Ricci, and all the technical contributors who played a vital role in this project. This work was partially funded by the European Union's Horizon 2020 Framework Program under Grant Agreement #951974, as well as by NEMC-Italy, Innovationgen Srl-Italy, and the Anthropocene Institute-USA.

We also express our sincere appreciation to Jed Rothwell for his valuable revisions, which significantly enhanced the English and overall readability of our manuscript. Lastly, we wish to thank the anonymous referee, whose insightful suggestions greatly clarified several ambiguous points and further improved the quality of this manuscript.

Disclaimer: This document represents the sole responsibility of the authors and may not necessarily reflect the opinions or positions of the entire CleanHME project.

8. Addendum A: A Typical Example of AHE Calculation, Using Deuterium Gas

Using calibration data with helium inside the reactor, we analyze the reactor's outer wall temperature (T_{ext}) relative to the ambient temperature (T_{ext}–T_a) while varying the input power (P_{in}) from 10 W to 150 W in 10 W increments. A fitting procedure is applied to derive a fourth-degree equation that correlates input power to the reactor's external temperature at any specified temperature.

The same approach can be applied to data from an experiment with deuterium (D_2) in the reactor. By comparing the input power requirements for D_2 against the helium reference, we can subtract the two fitting functions, plotting temperature values on the x-axis for a clear comparison. Below is an example of a real test comparison:

Table A. Input Power (P_{in}) as a Function of Temperature for D_2 and He, and Excess Power Calculation

T_{ext}-T_a (He) [°C]	P_{in} (D_2) [W]	P_{in} (He) [W]	AHE (D_2 - He) [W]
30,67	9,91	9,98	0,07
55,50	19,74	19,88	0,13
76,69	29,74	29,97	0,23
95,75	39,30	39,86	0,56
113,64	48,43	49,62	1,19
130,88	57,23	59,41	2,17
147,64	65,79	69,32	3,53
163,83	74,17	79,39	5,23
179,22	82,42	89,63	7,21
193,52	90,57	99,93	9,36
206,51	98,62	110,18	11,56
218,12	106,54	120,23	13,69
228,53	114,40	130,13	15,73
238,29	122,57	140,30	17,73
248,41	132,02	151,90	19,88

To generate a graph of excess power as a function of temperature using Table 1, we plot the temperature differential (T_{ext}–T_a) on the x-axis and the calculated excess power values ($P_{in}(D_2)$–$P_{in}(He)$) on the y-axis.

When interpreting these results, it is essential to account for a common observation: artifacts may stem from the differences in thermal conductivity between helium (He) and deuterium (D_2). The thermal conductivities of these gases at 1 atmosphere and room temperature [30] are presented below. For gas mixtures, conductivity values were calculated using the semi-empirical Wassiljewa equation [31], which provides a reliable estimate of the effective thermal conductivity based on the properties of each component.

- **He**: 0.1567 W/m·K
- **H_2**: 0.186 W/m·K
- **D_2**: 0.135 W/m·K
- **Ar**: 0.0177 W/m·K [32]

The higher thermal conductivity of helium relative to deuterium suggests that helium could lead to increased heat losses at the reactor's extremities, thus requiring a greater input power (P_{in}) to maintain equivalent temperature conditions. This introduces a potential source of concern, as the observed differences in input power between He and D_2 may partly stem from such thermal losses rather than strictly indicating Anomalous Heat Excess (AHE).

We have previously addressed this observation by confirming our thermometric evaluations of AHE using an airflow calorimeter [33]. While this method is more robust against criticisms and potential artifacts, it is important to

Table B. This table presents the experimentally determined thermal conductivities of helium, hydrogen, deuterium, and argon (highlighted in **bold red** for clarity) at 25 °C. Conductivity values at elevated temperatures, as well as those for **50:50 volumetric mixtures** (Ar-He, Ar-H_2, Ar-D_2), have been estimated using the semi-empirical Wassiljewa equation, with a temperature dependence constant of n=0.67. While this approach has certain limitations, it provides a consistent basis for comparing thermal conductivity variations across temperatures for each gas and mixture. This comparative framework is especially valuable for examining thermal behaviors across a broad range of practical conditions, offering useful insights into their respective conductive properties.

Temperature (°C)	Helium	Hydrogen	Deuterium	Argon	Ar-He	Ar-H_2	Ar-D_2
25	**0.1567**	**0.186**	**0.135**	**0.0177**	0.045	0.049	0.046
200	0.2135	0.2534	0.184	0.0241	0.0613	0.0668	0.0627
300	0.2428	0.2882	0.2092	0.0274	0.0697	0.0759	0.0713
500	0.2967	0.3522	0.2556	0.0335	0.0852	0.0928	0.0871
700	0.3462	0.4109	0.2982	0.0391	0.0994	0.1082	0.1016

note that it requires significantly longer acquisition times for calorimetric measurements, which extends the duration of each experimental campaign.

In addressing these critiques, we emphasize that, during the initial H_2 gas injection stages in Fig. 4 (experiment #1), the values of AHE, normalized to He, were indeed lower. This is consistent with expectations, as the thermal conductivity of H_2 is higher than that of He or D_2, allowing for greater heat dissipation. The observed increase in ΔW at elevated temperatures strongly suggests that the role of gas thermal conductivity in affecting AHE results is minimal.

Moreover, the higher AHE values observed in H_2#4 indicate that the thermal behavior within the reactor is governed more by intrinsic active processes than by the thermal properties of the gases. This reinforces our assertion that the observed results reflect genuine effects, rather than artifacts from conductivity differences. These findings support the robustness of the observed phenomena and reduce the likelihood that variations in gas conductivity significantly influenced the data.

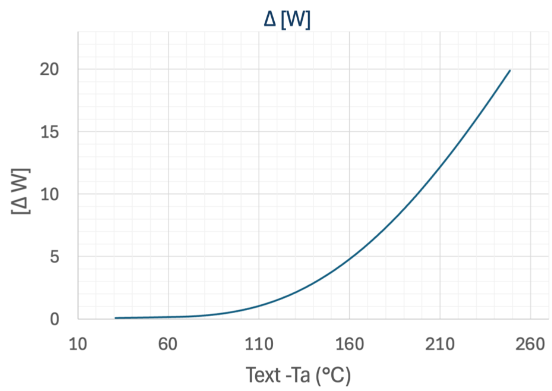

Figure A. The ΔW values (assumed to closely approximate AHE) between helium (He) and deuterium (D_2) runs are analyzed as a function of the temperature difference between the reactor's outer wall and ambient (T_{ext}–T_a). This approach allows for direct comparison of AHE behavior under different gas conditions, highlighting temperature-dependent variations that may reveal underlying differences in thermal interactions within the reactor.

9. Addendum B: Comprehensive Electrical Characterization During Stimulation with Direct Current, Unipolar, and Symmetric Sinusoidal Waveforms

Table C. Overview of Direct Current (DC), Unipolar Negative (UN), Unipolar Positive (UP), and Symmetric Sinusoidal 50 Hz (SS). The reactor was loaded at room temperature with 3 bars of a 50:50 volumetric mixture of hydrogen and argon. The experiment was conducted between October 19, 2023, and November 13, 2023. The following parameters were used to analyze the electrical signals or waveforms:

- **Type:** The type of electrical signal or waveform being analyzed.
- **Pw (W):** Power in watts (W) applied during the experiment.
- **Vrms (V):** Root-mean-square voltage in volts (V), representing the effective voltage.
- **Vpk (V):** Peak voltage in volts (V), indicating the maximum voltage level reached in the waveform.
- **Irms (A):** Root-mean-square current in amperes (A), representing the effective current.
- **Ipk (A):** Peak current in amperes (A), indicating the maximum current level reached in the waveform.
- **Vk (V):** Voltage across the counter electrode and ground.
- **Ik (μA):** Maximum current in microamperes (μA) flowing through the counter electrode when short-circuited.
- **Vpk/Pw:** The ratio of peak voltage to power, representing the efficiency of the electromigration effect along the wire. A higher ratio signifies greater efficiency.
- **Vrms/Irms:** The ratio of root-mean-square voltage to root-mean-square current, representing the resistance (Ohms) in the circuit.

Type; Pw(W);	Vrms(V)	Vpk(V)	Irms(A)	Ipk(A)	Vk(V)	Ik(A)	Vpk/Pw	Vrms/Irms (Ohm)
DC; 0.9466	−4.815	−4.815	−0.1966	−0.1966	0	0	5.0866	24.491
DC; 184.7	−68.96	−68.96	−2.6784	−2.6784	−17.16	−41	0.3773	25.746
DC; 171.66	−66.31	−66.31	−2.5889	−2.5889	−15.59	−20.8	0.3863	25.613
DC; 157.38	−63.29	−63.29	−2.4867	−2.4867	−13.31	−9.2	0.4021	25.451
DC; 149,61	−61.62	−61.62	−2.428	−2.428	−11.679	−5.8	0.4119	25.379
DC; 141.21	−59.74	−59.74	−2.3638	−2.3638	−10.08	−3.6	0.4231	25.273
DC; 121.19	−55.08	−55.08	−2.2002	−2.2002	−5.66	−1.2	0.4519	25.034
DC; 101.46	−50.15	−50.15	−2.0231	−2.0231	−3.01	−0.3	0.4943	24.788
DC; 79.801	−44.16	−44.16	−1.8071	−1.8071	−0.978	0	0.5534	24.444
DC; 59.65	−37.884	−37.884	−1.5746	−1.5746	−0.14	0	0.6351	24.059
DC; 40.16	−31.043	−31.043	−1.2937	−1.2937	−0.093	0	0.7730	23.996
DC; 20.1758	−21.99	−21.99	−0.9175	−0.9175	−0.004	0	1.0990	23.967
DC; 9.77658	−15.307	−15.307	−0.6387	−0.6387	−0.001	0	1.5657	23.965
DC; 0.9821	−4.85	−4.85	−0.2025	−0.2025	0	0	4.9384	23.951
UN; 100	−50.4	−100	−2.03	−4.2	−12.5	−5.8	1	24.827
UN; 148	−62.1	−126	−2.46	−4.9	−13.94	−16	0.85	25.24
UN; 153	−63.6	−128	−2.49	−5.0	−15.79	−19.3	0.8366	25.54
UN; 168	−66.6	−134	−2.6	−5.2	−14.43	−26.6	0.7976	25.615
UN; 183	−69.7	−140	−2.7	−5.4	−13.12	−15.2	0.765	25.815
UN; 170	−67	−132	−2.62	−5.3	−14.56	−23	0.7764	25.57
UP; 170	65.2	130	2.53	50.	34.52	240	0.7647	25.7707
UP; 183	67.9	135	2.62	5.2	38.8	400	0.7377	25.916
UP; 153	61.3	120	2.42	4.8	30.35	116	0.7843	25.33
UP; 129	55.7	110	2.25	4.45	18.92	34	0.8527	24.755
UP; 109	51.6	105	2.07	4	14.5	11.8	0.9633	24.927
UP; 101.7	49.9	100	1.99	4	15.5	8.8	0.98328	25.075
UP; 81.2	44.5	88	1.8	3.5	9.82	3.6	1.0837	24.722
UP; 59.4	37.2	73	1.55	3	4.81	1.4	1.2289	24
UP; 40.5	31	60.5	1.28	2.5	2.7	0.7	1.4938	24.218
UP; 20.4	21.9	43	0.9	1.75	0.94	0.8	2.1078	24.33

Table C. Continued

Type; Pw(W);	Vrms(V)	Vpk(V)	Irms(A)	Ipk(A)	Vk(V)	Ik(A)	Vpk/Pw	Vrms/Irms (Ohm)
UP; 162.5	63.5	125	2.47	5	30.5	140	0.7692	25.708
UP; 10.45	15.7	32	0.647	1.28	0.537	1	3.062	24.2658
DC; 0.9597	−4.818	−4.818	0.1992	0.1992	NA	NA	5.020	24.1867
SS; 170.5	66.1	+−92	2.59	+−3.8	+−35.2	290	0.53958	25.52
SS; 150	61.8	+−86	2.43	+−3.55	+−33	145	0.5733	25.432
SS; 133	57.8	+−81	2.3	+−2.4	+−29.9	65	0.609	25.13
SS; 110	52.4	+−76	2.09	+−3	+−26.4	28.1	0.6909	25.0717
SS; 102	50.6	+−72	2.02	+−2.95	+−22.6	16.7	0.70588	25.049
SS; 83	45.1	+−64	1.86	+−2.6	+−14.4	5.2	0.77108	24.247
SS; 61	38.7	+−55	1.58	+−2.3	+−7.4	1.6	0.9016	24.4936
SS; 40	31.1	+−44	1.28	+−1.8	+−3.57	0.8	1.1	24.2968
SS; 19.7	21.8	+−31	0.9	+−1.3	+−1.23	0.7	1.5736	24.22
DC; 0.95	−4.77	−4.77	−0.199	−0.199	NA	NA	5.021	23.946

It is important to note that after completing each series of Unipolar Positive (UP) and Symmetric Sinusoidal (SS) experiments, an additional experiment using Direct Current (DC) was conducted. This DC test was essential for verifying data consistency and establishing a reference baseline. By cross-referencing the results obtained from the different waveform stimulations, we ensured the reliability and accuracy of the experimental data.

References

[1] F. Celani, A. Spallone, P. Tripodi, A. Petrocchi, D. d. Gioacchino, M. Boutet, P. Marini, V. D. Stefano, M. Diociaiuti and W. Collis, “Reproducible D/Pd Ratio >1 and Excess Heat Correlation by 1-μs-Pulse, High-Current Electrolysis,” *Fusion Technology,* vol. 29, no. 3, pp. 398–404, 1996.

[2] F. Celani, A. Spallone, P. Tripodi, A. Petrocchi, D. Di Gioacchino, P. Marini, V. Di Stefano, S. Pace and A. Mancini, “Deuterium overloading of palladium wires by means of high power μs pulsed electrolysis and electromigration: suggestions of a “phase transition” and related excess heat,” *Physics Letters A,* vol. 214, no. 1–2, pp. 1–13, 6 May 1996.

[3] F. Celani, C. Lorenzetti, E. Purchi, S. Fiorilla, C. Stefano, M. Nakamura, P. Cerreoni, E. Marano and A. Spallone, “Electromagnetic Excitation of Coaxially-Coiled Constantan Wires by High-Power, High-Voltage, Microsecond Pulses,” *Journal of Condensed Matter Nuclear Science,* vol. 36, p. 408–435, 2022.

[4] F. Celani, C. Lorenzetti, G. Vassallo, E. Purchi, S. Fiorilla, S. Cupellini, M. Nakamura, P. Cerreoni, P. Boccanera, R. Burri and A. Spallone, “Progress Toward an Understanding of LENR-AHE Effects in Coated Constantan Wires in D_2 Atmosphere: DC/AC Voltage Stimulation,” *J. Condensed Matter Nucl. Sci.,* vol. 33, p. 1–28, 2020.

[5] Y. Fukai and N. Ōkuma, “Formation of Superabundant Vacancies in Pd Hydride under High Hydrogen Pressures,” *Physical Review Letters,* vol. 73, no. 1640, 1994.

[6] F. Celani, G. Vassallo, E. Purchi, S. Fiorilla, L. Notargiacomo, C. Lorenzetti, A. Calaon, B. Ortenzi, A. Spallone, M. Nakamura, A. Nuvoli, P. Cirilli, P. Boccanera and S. Pella, “Improved stability and performance of surface-modified Constantan wires, by chemical additions and unconventional geometrical structures,” *J. Condensed Matter Nucl. Sci.,* vol. 27, pp. 9–21, 2018.

[7] F. Celani and C. Lorenzetti, “Chapter 7 - Electrically induced anomalous thermal phenomena in nanostructured wires,” in *Cold Fusion*, 2020 ed., Amsterdam, Elsevier, 2020, pp. 101–113.

[8] F. Celani, C. Lorenzetti, G. Vassallo, S. Cupellini and S. Fiorilla, “Effects “of super-Capuchin knot” geometry, and additional electric fields, on Hydrogen/Deuterium absorption: related AHE on long and thin Constantan wires with sub-micrometric surfaces at high temperatures.,” in *2019 LANR/CF Colloquium at MIT-USA*, Cambridge MA 02139 (USA), March 23–24, 2019.

[9] F. Celani, C. Lorenzetti, G. Vassallo, E. Purchi, S. Fiorilla, S. Cupellini, M. Nakamura, P. Cerreoni, R. Burri, A. Spallone and E. Marano, "Advancements in the Production of Anomalous Heat Effect in Constantan Wires: Developing a Robust Experimental Protocol," *J. Condensed Matter Nucl. Sci.,* vol. 38, pp. 211–224, 2024.

[10] M. R. Staker, "Estimating volume fractions of superabundant vacancy phases and their potential roles in low energy nuclear reactions and high conductivity in the palladium – isotopic hydrogen system," *Materials Science and Engineering: B,* vol. 259, 2020.

[11] M. R. Staker, "How to achieve the Fleischmann-Pons heat effect," *International Journal of Hydrogen Energy,* vol. 48, no. 5, pp. 1988–2000, 2023.

[12] M. R. Staker, "The role of superabundant vacancy delta to delta prime transformation in stopping Fleischmann-Pons heat effect in palladium-deuterium," *International Journal of Hydrogen Energy,* vol. 48, no. 40, pp. 15195–15202, 2023.

[13] W. Brückner, S. Baunack, G. Reiss, G. Leitner and T. Knuth, "Oxidation behavior of Cu-Ni(Mn) (constantan) films," *Thin Solid Films,* vol. 258, no. 1-2, p. 252, 1995.

[14] F. Celani and A. Spallone , "High power μs pulsed electrolysis for high deuterium loading on Pd plates," in *Selected papers following ICCF4, Dec. 6-9, 1993*, Maui-Hawaii, 1994.

[15] F. Celani and A. Spallone, "High power μs pulsed electrolysis using palladium wires: evidence for a possible "phase" transition under deuterium overloaded conditions and related excess heat," in *Proceedings from ICCF5, 9-13 April 1995*, Montecarlo.

[16] T. N. Claytor, P. A. Seeger, R. K. Rohwer, D. G. Tuggle and W. R. Doty, "Tritium and Neutron Measurements of a Solid State Cell," Los Alamos National Laboratory, Washington, 1989.

[17] T. N. Claytor, D. D. Jackson and D. G. Tuggle, "Tritium Production from a Low Voltage Deuterium Discharge on Palladium and Other Metals," *Journal of New Energy,* vol. 1, no. 1, pp. 111–118, 1996.

[18] T. N. Claytor, D. G. Tuggle and H. O. Menlove, "Tritium Generation and Neutron Measurements in Pd-Si Under High Deuterium Gas Pressure," in *Presented at the 2nd Annual Conference on Cold Fusion, Como, Italy, June 29 - July 4, 1991.*

[19] D. G. Tuggle, T. N. Claytor and S. F. Taylor, "Tritium Evolution from Various Morphologies of Palladium," Los Alamos National Laboratory, 1994.

[20] J. Dufour, D. Murat, X. Dufour and J. Fos, "Exothermic reaction induced by high density current in metals – Possible nuclear origin," *Annales de la Fondation Louis de Broglie,* vol. 29, no. Hors série 3, pp. 1081–1092, 2004.

[21] J. Dufour , J. Foos and J. P. Millot, "Cold Fusion by Sparking in Hydrogen Isotopes. Energy Balances and Search for Fusion By-products. A Strategy to Prove the Reality of Cold Fusion," in *Fourth International Conference on Cold Fusion*, Lahaina, Maui, 1993.

[22] Y. Iwamura, T. Itoh, M. Sakano, S. Sakai and S. Kuribayashi, "Low Energy Nuclear Transmutation in Condensed Matter induced by D_2 Gas Permeation through Pd Complexes: Correlation between Deuterium Flux and Nuclear Products," in *Proc. of ICCF10, Condensed Matter Nuclear Science*, Cambridge, MA, 2006.

[23] Y. Iwamura, T. Itoh and N. Gotoh, "Characteristic X-Ray and Neutron Emission from Electrochemically Deuterated Palladium," in *Proc. 5th Int. Conf. Cold Fusion, Monte Carlo*, Monaco, 1995.

[24] Y. Iwamura, T. Itoh and M. Sakano, "Nuclear products and their time dependence induced by continuous diffusion of deuterium through multi-layer palladium containing low work function material," in *8th International Conference on Cold Fusion*, Lerici (La Spezia), 2000.

[25] T. O. Passell, "Use of Helium Production to Screen Glow Discharges for Low Energy Nuclear Reactions (LENR)," in *American Physical Society. APS March Meeting 2011. March 21-25 2011. Abstract ID Y33.008.*

[26] R. L. Mills and P. Ray, "Spectral emFractional quantum energy levels of atomic hydrogen from a helium–hydrogen plasma and the implications for dark matter," *International Journal of Hydrogen Energy,* vol. 27, no. 3, pp. 301–322, 2002.

[27] R. L. Mills, W. R. Good, J. Phillips and A. I. Popov, "Lower-energy hydrogen methods and structures". Patent US6024935A, 1997.

[28] D. Alexandrov, "Entering the Hot Case of Cold Nuclear Fusion," Elsevier, 5 June 2023. [Online]. Available: https://doi.org/10.2139/ssrn.4469848. [Accessed 10 January 2024].

[29] D. Alexandrov, "Low-energy nuclear fusion reactions in solids: Experiments," *International Journal of Energy Research,* vol. 45, no. Issue8 - Special Issue: Progress in Emerging Nuclear Energy Systems, pp. 12234–12246, 8 June 2021.

[30] P. J. Linstrom and W. G. Mallard, NIST Chemistry WebBook, vol. NIST Standard Reference Database Number 69, N. I. o. S. a. Technoloy, Ed., https://webbook.nist.gov/chemistry/, 2024.

[31] R. C. Reid, J. M. Prausnitz and B. E. Poling, The Properties of Gases and Liquids (4th ed.), New York: McGraw-Hill, 1987.

[32] Y. S. Touloukian, TPRC Data Series: Thermal Conductivity of Pure Gases, Purdue University, 1967.

[33] F. Celani, C. Lorenzetti, A. Spallone, G. Vassallo, E. Purchi, L. Notargiacomo and R. Burri, "Steps to Identify Main Parameters for AHE Generation in Sub-micrometric Materials: Measurements by Isoperibolic and Air-flow Calorimetry," *Journal of Condensed Matter Nuclear Science,* vol. 29, pp. 52–74, 2019.